

# Literature review: synthesis of CuO (Copper Oxide) nanoparticles for thermal energy storage

Clarysa Satari, Rahmi Sabila Sidqi, Rian Febriyana Putra, Silmi Ridwan Putri, Asep Bayu Dani Nandiyanto\*

Departemen Kimia, Universitas Pendidikan Indonesia, Jl. Dr. Setiabudi no 229, Bandung 40154, Jawa Barat, INDONESIA

Email\*: [nandiyanto@upi.edu](mailto:nandiyanto@upi.edu)

**Abstract** – This paper aims to provide a discussion of the methods used in the synthesis of CuO nanoparticles. A review of the CuO nanoparticle synthesis method was carried out from 65 articles from 2000 to 2021. The CuO nanoparticle synthesis methods described in this paper are electrochemical, sonochemical, sol-gel, biogenic, green synthesis, and hydrothermal methods. Each method used to synthesize CuO nanoparticles has advantages and disadvantages. Based on their advantages, electrochemical, sonochemical, green synthesis, and biogenic methods are environmentally friendly methods. Moreover, the hydrothermal and biogenic methods are simple methods with easy preparation. In its utilization, CuO nanoparticles can be used to divert heat energy. The addition of a volume of CuO nanoparticles into the nitrate salt can increase the thermal diffusivity and thermal conductivity used in solar power plants. Among the methods described, the hydrothermal method is the most effective and efficient technique. This is because the method is simple (without using any surfactant template), easy to vary the temperature, reactant concentration, and time variables on the growth of nanostructures. This paper is expected to provide some considerations regarding the synthesis method of CuO nanoparticles that can be used on an industrial scale based on the advantages of each method.

**Keywords:** CuO nanoparticles; Synthesis methods; Literature review

Received: 11/07/2021 – Accepted: 15/11/2021

## I. Introduction

Nanotechnology in Indonesia has been developed since 2004. Until now, Indonesia has produced various nanotechnology-based products in various fields including agriculture, food, textile, automotive, household, oil, cosmetics, health, renewable energy, and other industries [1]. Currently, many studies focused more on nanoparticle research. This is because nanoparticles have several advantages, namely cheap, high yield under mild reaction conditions, high surface area, being physically stable, and reducing reaction time [2].

One of the nanotechnology products in Indonesia is CuO nanoparticles. CuO (Copper Oxide) nanoparticles are one of the transition metal oxide nanoparticles that have become highly desirable materials for many applications. Metal oxides are generally characterized by a very wide bandgap [3] whereas CuO nanoparticles are p-type oxide semiconductors with a bandgap of 1.2 - 1.5 eV [4]. One of the uses of nanoparticles is in solar cells [3]. Solar power or solar cells is one viable source of sustainable energy. However, like many renewable

energy technologies, the self-conversion of solar energy suffers from shortages due to intermittent solar resources [5]. Molten salt has potential as a Heat Transfer Fluid (HTF) and thermal storage in solar power plants. However, organic HTF is very unstable at high temperatures. Thus, the addition of CuO nanoparticles to it will increase the stability in the highly oxidative liquefaction of nitrate salts [6].

In addition, CuO nanoparticles have unique catalytic, optical, and electrical properties [7]. The unique properties of these particles allow CuO nanoparticles to be applied in various fields [8], such as photocatalytic reactions [9-10], antibacterial activity [11-16], non-enzymatic glucose sensor [17], polymer solar cells [18], inertness sensor [19], oxide architectural pores [20], ammonia sensing [21], antifungal agents [22], and CuO nanoparticles are also used in dry cell batteries and animal feeding supplements to combat copper deficiency.

The methods that can be used in the synthesis of CuO nanoparticles include electrochemical methods [12], sonochemistry [23], sol-gel [24], green synthesis [25], hydrothermal [26], and biogenic [27]. Each method has its advantages and has different results so it is necessary to do a review.

Therefore, the purpose of this paper is to provide a discussion of several methods of synthesizing CuO nanoparticles based on their advantages and disadvantages to obtain a more effective and efficient method of synthesizing CuO nanoparticles. This paper is expected to provide an overview of the manufacture of CuO nanoparticles and help provide some considerations to be applied on the industrial scale for the manufacture of CuO nanoparticles. Several analysis methods were also added, including X-Ray diffraction (XRD), scanning electron microscope (SEM), transmission electron microscope (TEM), Fourier transform infra red (FT-IR), and so on.

## II. Study on Methods in The Synthesis of CuO (Copper Oxide)

Table 1 shows several methods of synthesizing CuO (Copper Oxide) nanoparticles along with their synthesis results, weaknesses, and strengths. Methods that can be used to synthesize CuO nanoparticles are electrochemical, sonochemical, sol-gel, green synthesis, biogenic, and hydrothermal methods.

Table 1. Methods in the synthesis of CuO nanoparticles

Ref	Material	Method	Result	Advantage	Disadvantages
[12]	Copper sheet (anode), platinum sheet (cathode), TBAB (electrolyte)	Electrochemical	The absorption band of CuO nanoparticles is in the range of 550-600 nm. The copper particles show a height of about 570 nm. In the IR spectrum, the peak appears at $3298\text{ cm}^{-1}$ . Microstructure SEM of the electrochemical reduction of copper oxide nanoparticles showing solid agglomeration. The shape is irregular with the non-uniform distribution. HRTEM showed spherical CuO nanoparticles with a size of 5-10 nm and a monoclinic structure.	Environmentally friendly and efficient in providing new opportunities for the rapid screening of various metal nanoparticle syntheses as well as for the development of new drugs for materials scientists	The reaction that occurs can cause a layer (double layer) attached to the outside of the electrode to increase the resistance that occurs and reduce the current.
[23]	$\text{CuN}_2\text{O}_6 \cdot 3\text{H}_2\text{O}$ and NaOH	Sonochemistry	CuO particles obtained by the reaction of fewer than 20 minutes have a particle size of 80 nm. Meanwhile, the 30-minute reaction resulted in particle size of 45 nm. Extended time will result in particle size which tends to increase. An increase in the calcination temperature leads to complete CuO crystallization, accompanying well-defined and uniform crystalline particles with a particle size of ~50-70 nm.	Environmentally friendly, easy to prepare at low temperatures, minimal by-products.	Uneven distribution of particles
[24]	Glacial acetic acid and $\text{CuCl}_2 \cdot 2\text{H}_2\text{O}$	Sol-gel	SEM shows the heterogeneous distribution of the synthesized CuO nanoparticles. XRD pattern of CuO nanoparticles shows a single phase with a monoclinic structure. The mole ratio controls the size of the CuO nanoparticles. The size of CuO nanoparticles is 16 nm.	Can be carried out at room temperature and accurately control chemical and physical characteristics.	Relatively long processing time.
[25]	<i>Ixora coccinea</i> and $\text{CuSO}_4 \cdot 5\text{H}_2\text{O}$	Green Synthesis	Mean size of CuO nanoparticles 300 nm (SEM), 80-110 nm (TEM) It was found that ultrasonication improves the distribution of nanoparticles in the liquid by preventing cluster formation. The Green synthesis method is a biologically reliable process that has been established for the synthesis of CuO nanoparticles.	Environmentally friendly, low cost, and non-toxic synthesis method, produces large-scale nanoparticles.	The raw materials are hard to find.
[26]	Ethanol, NaOH, and $\text{Cu}(\text{CH}_3\text{COO})_2$	Hydrothermal	The results showed that the CuO nanoparticle structure has a monoclinic structure with a single crystal phase. The structure and morphology of CuO nanocrystals can be controlled by changing the concentration of the reactants. The rate of heat degradation to methylene blue can reach 92.1%.	Simple (without using any surfactant template), it is easy to vary the variables of temperature, reactant concentration, and time on the growth of nanostructures. Particle size and shape can be controlled.	Equipment costs are expensive, it is difficult to control the stoichiometry of the solution, hydrothermal slurries are corrosive, and the use of high-pressure vessels will be dangerous in the event of an accident.
[27]	young guava leaves, $\text{Cu}(\text{CH}_3\text{COO})_2 \cdot \text{H}_2\text{O}$	Biogenic	The particle size of CuO nanoparticles is 11.07 nm. CuO nanoparticles show excellent degradation efficiency for industrial dyes, namely Nile blue (NB). As well as CuO catalysts were found to be reusable for photocatalytic dye degradation.	Simple, eco-friendly, and economical.	Difficult implementation on a large scale and the need in maintaining cell cultures, control size, shape, and crystallinity.

### III. Synthesis of CuO Nanoparticles

CuO nanoparticles can be synthesized by several methods. Review is needed to compare which method is more effective and efficient. The review of the CuO nanoparticle synthesis method was carried out from 65 articles from 2000 to 2021. Based on the synthesis method that has been reviewed, there are several kinds of nanoparticle synthesis methods, namely electrochemical, sonochemical, sol-gel, green synthesis, hydrothermal, biogenic.

## IV. Result and Discussion

### IV.1. Electrochemical Method

The electrochemical method is one of the many available methods for synthesizing metal oxides in the nanodomain due to its simplicity, low-temperature operation, and commercial feasibility [28]. Electrochemical is a method based on oxidation-reduction (redox) reactions. Electrochemical systems include electrochemical cells and electrochemical reactions [29]. The basic equipment of electrochemical is to use two electrodes and an electrolyte solution in the process. Overall the electrochemical method uses two inexpensive electrodes. The bulk metal used as anode will be converted into a metal group which in this case is Cu. Tetrabutylammonium bromide (TBAB) in the electrolyte is used as a stabilizer. The electrochemical method is a process in which bulk metal is oxidized at the anode and metal cations will migrate to the cathode resulting in reduction with the formation of metal or metal oxide in a zero oxidation state. Agglomeration with the formation of unwanted metal powders is prevented by the presence of an ammonium stabilizer. The anode will dissolve slowly and lead to the formation of then passivation with active TBAB [12].

The electrodes used in the synthesis of CuO nanoparticles are copper sheet (anode) and platinum sheet (cathode). The electrolyte used was 0.01 M tetrabutylammonium bromide (TBAB) and acetonitrile in a ratio of 4:1. The current used is 6 mA/cm<sup>2</sup>. Electrolysis is carried out in a nitrogen atmosphere. The resulting copper oxide nanoparticles will be dark brown [12].

The obtained nanoparticles must be characterized, this is to find out that the nanoparticles obtained are the desired CuO nanoparticles. The characterization of nanoparticles can be done using UV-Visible [4, 12, 30], FT-IR spectrophotometer [7, 4, 31-32], XRD [4, 7, 10, 12], and SEM [4, 10, 12]. UV-Visible can be used to determine when the precursor turns into CuO nanoparticles. The maximum absorption bands reported are 550-600 nm [12] and 638-642 nm [4]. This absorption band is closely related to the surface plasmon resonance peak of CuO nanoparticles.

The peaks of the IR spectrum that appeared were reported with different results from one researcher to another. The reported IR spectrum peak is 3424-3437

cm<sup>-1</sup> which can be attributed to the hydroxyl group which is the hygroscopic nature of CuO nanoparticles [4]. The characteristics of CuO nanoparticles using an FT-IR spectrophotometer can be shown in Figure 1.

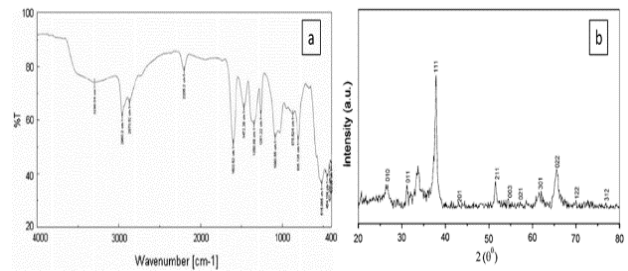


Figure 1. (a) IR spectra pattern of CuO nanoparticles with TBAB 0.01 M, (b) X-ray diffraction pattern of CuO nanoparticles using TBAB [12].

The average particle size of the synthesized nanoparticles was characterized by XRD and TEM. XRD results of CuO nanoparticles showed that the calculated average particle size was 5-10 nm [12]. Figure 2 shows the HRTEM results of CuO nanoparticles which are spherical and 5-10 nm in size [12]. Other studies reported that the average particle size obtained was 5-30 nm [4, 31] and had a monoclinic structure [4, 12, 31]. These results were confirmed by XRD and TEM. In addition, CuO nanoparticles measuring 4.0 nm have been reported to have been successfully synthesized [7]. The size and nanoparticles of copper oxide depend on several parameters used (electrode, electrolyte, temperature, electrolysis time, current, solution, and cell shape dimensions).

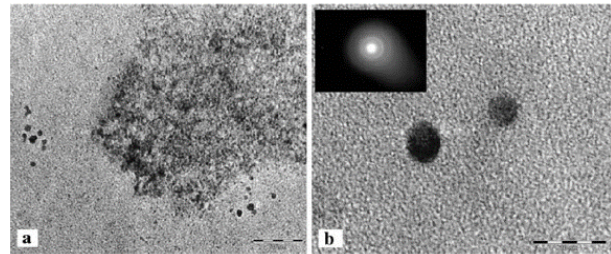


Figure 2. HRTEM CuO nanoparticles are spherical and 5-10 nm in size [12].

The surface morphology of CuO nanoparticles was investigated using an SEM. SEM microstructure of electrochemical reduction derived from copper nanoparticles shows solid agglomeration [4,12]. SEM microstructure of CuO nanoparticles is shown in Figure 3.

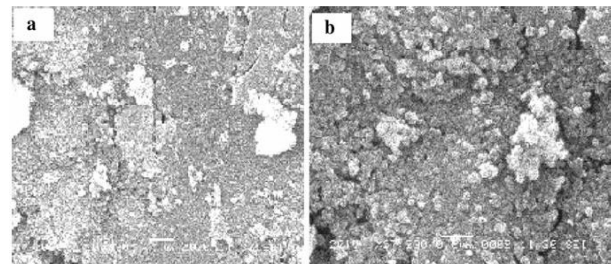


Figure 3. SEM of CuO nanoparticles covered with 0.01 M TBAB [20].

The electrochemical method is an easy and less time-consuming method with the highest nanoparticle purity [4]. In addition, the electrochemical process is environmentally friendly and provides new opportunities for the synthesis of metal nanoparticles. The electrochemical method is considered good for use as new drug development. Although the electrochemical method has several advantages, this method also has several disadvantages, namely, the reaction that occurs can cause a layer (double layer) to be attached to the outside of the electrode so that it increases the resistance that occurs and reduces the current [12].

#### IV.2. Sonochemical Method

Sonochemistry is a method of synthesizing materials using sound energy to induce physical and chemical changes in a liquid medium. The chemical effect of ultrasound produces acoustic cavitation, which is the formation and growth of foam in the liquid. The frequency used in the sonochemical method is a frequency in the range of 20 kHz - 2 MHz [29]. The basic principle of the sonochemical method is the displacement of sound waves that form and collapse the bubbles resulting in a local increase in temperature and pressure, causing physical and chemical changes in the material [33]. The schematic of the equipment used in the sonochemical method is shown in Figure 4.

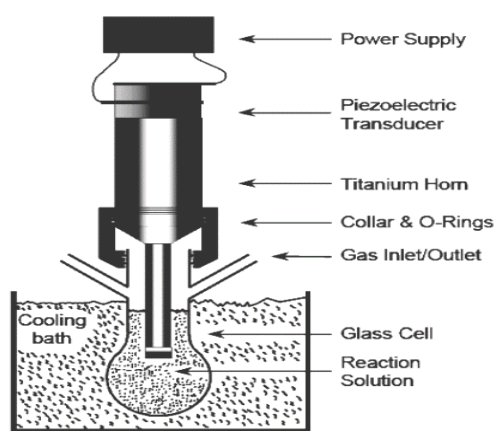


Figure 4. Schematic of Sonochemical Method Equipment [29].

The materials used in the synthesis of CuO nanoparticles by sonochemical methods are copper nitrate trihydrate ( $\text{Cu}(\text{NO}_3)_2 \cdot 3\text{H}_2\text{O}$ ) and sodium hydroxide (NaOH) with polyvinyl as the initial precursor [23]. Synthesis of CuO nanoparticles begins by dissolving NaOH in deionized water. The resulting solution is then added to  $\text{Cu}(\text{NO}_3)_2 \cdot 3\text{H}_2\text{O}$  for 30 minutes slowly drop by drop. Sonication was carried out with the VCX 750 model. Several other researchers used different models in sonication such as the Branson 102C [33] and the ultrasound-assisted chemical reduction model UC-20A [8]. Sonication is carried out until the desired product is completely precipitated. The precipitated product was then calcined at different temperatures in the range of

400-700 °C for 2 hours. The thermal behavior of the product was investigated by Thermogravimetry (TG) powder in the open air with the heating rate used was 10 °C/min [23].

Characterization is done through several instruments. To characterize the structural and microstructural properties of CuO nanoparticles an X-ray diffractometer was used which in this synthesis used Panalytical x'Pert Pro MPD with radiation used was Cu-K $\alpha$  operating at 40 kV and 30 mA, respectively. The SEM (Scanning Electron Microscope) used is the JEOL JSM-6510 model [23].

Thermo-gravimetric and thermal-differential analysis of CuO nanoparticles were sonicated for 30 minutes. In this sonication, it is seen that there are 2 weight losses at a temperature of 180-250 °C and at a temperature of 500-700 °C as shown in Figure 5. The first decrease is due to evaporation of polyvinyl alcohol and deionization in the mixed solution while the second decrease is due to oxidation of copper metal in the air. resulted in the crystallization of CuO [23].

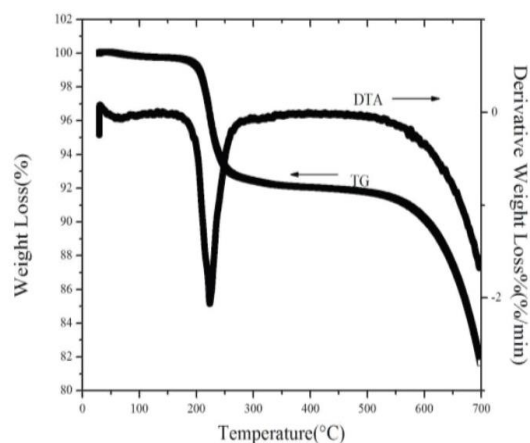


Figure 5. TG and DTA curves of the precipitated product sonicated for 30 minutes [33].

The diameter of CuO nanoparticles obtained by sonochemical methods is 50 nm [19]. These results have been confirmed by TEM (Transmission Electron Microscope) and SEM (Scanning Electron Microscope). With a similar method, CuO nanoparticles can also be produced which are 80 nm before calcination and 70 nm after being calcined at 500 °C for 2 hours [34]. The results of the calcination of the sample at a temperature of 400-500 °C and the XRD pattern of the sample showed that good CuO particle powder was only obtained by a sonochemical process [23]. The results of XRD (X-Ray Diffraction) CuO nanoparticles calcined and sonicated at different temperatures and times are shown in Figures 6 and 7.

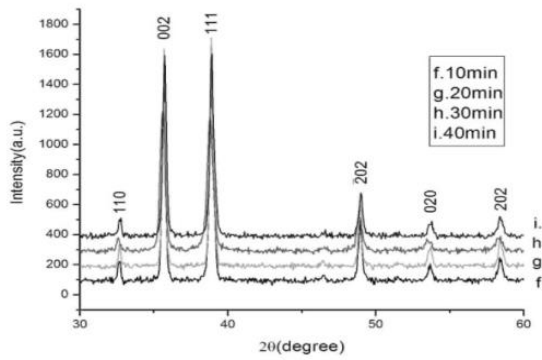


Figure 6. XRD pattern of calcined CuO nanoparticles at different temperatures [23].

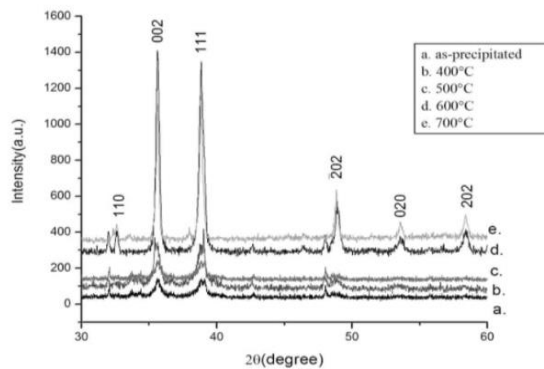


Figure 7. XRD Pattern of sonicated at different times [23].

The size of the CuO nanoparticles obtained can be influenced by the sonication time carried out as well as the Kalisani temperature. A longer sonication time will result in smaller particle size compared to a lower sonication time. CuO nanoparticles obtained by the reaction of fewer than 20 minutes produce particles of about 80 nm, whereas if the reaction is prolonged to 30 minutes the resulting particle size is 45 nm. This result is thought to be due to sufficient energy supplied to the system by ultrasound after a certain time and can induce nucleation disintegration. The results will be inversely proportional in the sense that the size will increase after extending the sonication time to 40 minutes. This is thought to be due to changes in the crystal structure caused by the abundant energy of ultrasound after the critical time has elapsed [23]. The effect of temperature also causes changes in the size of the resulting particles. As the calcination temperature increases, the particle size will increase or increase. This is because the formation of crystallization of CuO nanoparticles is complete and well defined and uniform with a particle size of 50-70 nm [23]. Figure 8 shows the SEM results regarding the morphology of CuO nanoparticles at various calcination temperatures, namely 400, 500, 600, and 700 °C. The morphology of nanoparticles can be affected by the pH of the surfactant. When the pH is set to 8 the morphology looks like leaves while after the pH is raised to 11 the morphology changes to like a lumpy flower [33].

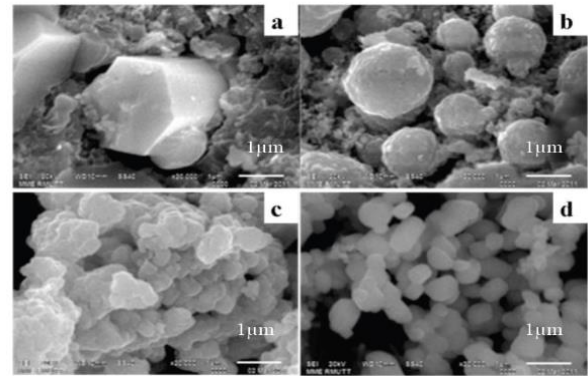


Figure 8. SEM morphology of CuO nanoparticles by sonochemical method calcined at various temperatures, namely 400, 500, 600, and 700 °C [23].

The sonochemical method has several advantages, namely easy preparation at low temperatures [18], can produce products with fine particles with nanometer dimensions [35], more uniform particle size distribution with higher phase purity. higher [33], reproducible [8], and the product can be used to remove environmental pollutants extensively [2]. The drawback of the sonochemical method is the uneven distribution of particles [23].

#### IV.3. Sol-gel Method

Another method for the synthesis of CuO nanoparticles is the sol-gel method [24, 36-39]. Synthesis of CuO nanoparticles the sol-gel method can use several reactants, including  $\text{CuCl}_2 \cdot 6\text{H}_2\text{O}$  [36], Lantana camara extract and  $\text{CuCl}_2 \cdot 2\text{H}_2\text{O}$  [37],  $[\text{Cu}(\text{CH}_3\text{COO})_2 \cdot \text{H}_2\text{O}]$  [38],  $\text{Cu}(\text{CH}_3\text{COO})_2$  with high purity [39], and glacial acetic acid and  $\text{CuCl}_2 \cdot 2\text{H}_2\text{O}$  [54]. The sol-gel method is carried out in several stages as shown in Figure 9.

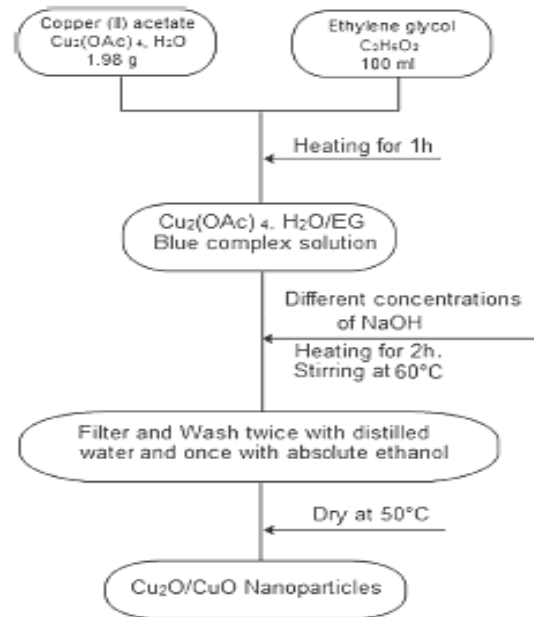


Figure 9. The process of making CuO nanoparticles using the sol-gel method [39].

The nanoparticle synthesis process using the sol-gel method started with glacial acetic acid added to  $\text{CuCl}_2 \cdot 2\text{H}_2\text{O}$  then heated to  $100\text{ }^\circ\text{C}$ . NaOH is added after mixing the reactants to make the pH equal to 7. The color of the stirred solution changes rapidly from green to black and a large amount of black precipitate forms immediately. The precipitate was centrifuged and washed with distilled water under vacuum and dried at room temperature [24]. NaOH was added to solutions of different concentrations at  $60\text{ }^\circ\text{C}$  and stirred for 2 hours then dried at  $50\text{ }^\circ\text{C}$  [39].  $\text{Cu}(\text{NO}_3)_2$  is dissolved in distilled water until dissolved. Then acetic acid was added to the solution and heated to  $100\text{ }^\circ\text{C}$  and stirred using a magnetic stirrer for 60 minutes, and acetic acid was then added with NaOH. The sole was heated and stirred for 1 hour then allowed to stand for 1 day. Centrifugation was carried out at 3000 rpm, and a bluish-green precipitate was obtained. Then the precipitate is annealed. Annealing was carried out at  $400\text{ }^\circ\text{C}$  for 4 hours then at  $1000\text{ }^\circ\text{C}$ , using a Lindberg furnace [40].

Characterization was carried out using several instruments such as XRD, TEM, and UV-Vis [39], FTIR in the range of  $4000.00$  to  $400.00\text{ cm}^{-1}$ , thermogravimetry with SDT Q 600, and SEM [40]. The structure and morphology of the synthesized CuO nanoparticles were investigated using XRD and SEM. The surface morphology of CuO nanoparticles was examined by SEM scanning with the nanostructures visible and showing the heterogeneous distribution of the synthesized CuO nanoparticles. The nanoparticle size in this method is  $16\text{ nm}$  and the nanoparticle size becomes smaller with increasing base concentration [24]. The result of the characterization of SEM is shown in Figure 10.

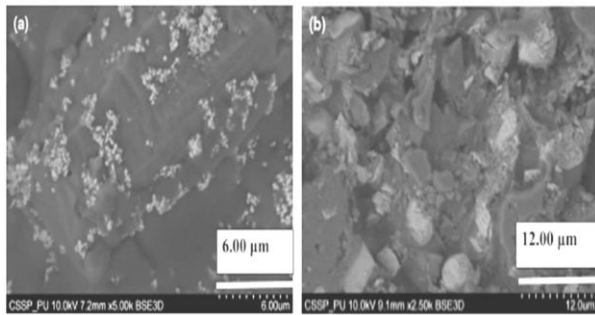


Figure 10. Surface morphology of CuO nanoparticles using SEM at (a)  $400\text{ }^\circ\text{C}$  and (b)  $1000\text{ }^\circ\text{C}$  [40].

XRD results show a single phase and a monoclinic structure. The intensity and peak position closely match the library data. The results of the characterization of XRD are shown in Figure 11 [39].

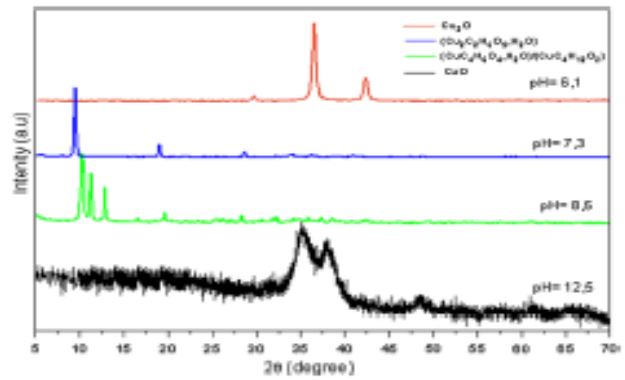


Figure 11. XRD pattern of samples prepared at various pHs [18].

The morphological and size distribution were examined by TEM. Figure 12 shows that the CuO nanoparticles are spherical with uniform distribution with an average diameter of  $4.5\text{ nm}$  [39].

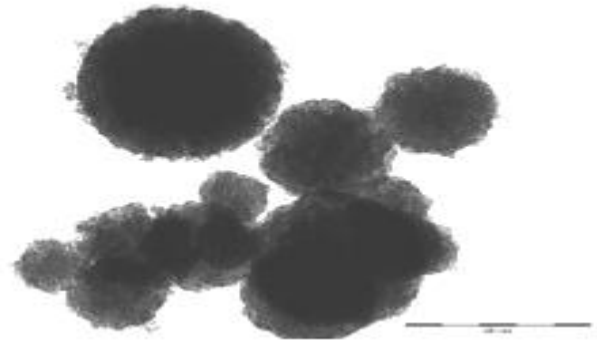


Figure 12. TEM results and particle size distribution of CuO nanoparticles [39].

Figure 13. FT-IR spectrum of CuO nanoparticles shows three peaks of the vibration of Cu-O observed at  $420.7$ ,  $472$ , and  $631.5\text{ cm}^{-1}$  [39].

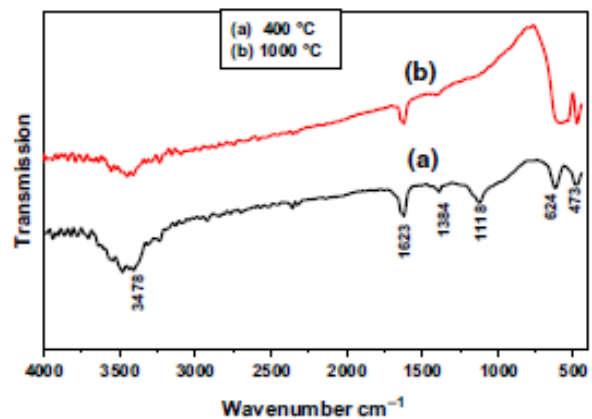


Figure 13. FT-IR spectrum of CuO nanoparticles at (a)  $400\text{ }^\circ\text{C}$  and (b)  $1000\text{ }^\circ\text{C}$  [40].

UV-Vis result is shown in Figure 14. As can be seen, an adsorption peak is observed at  $350\text{ nm}$ . The calculated band gap values are  $4.08\text{ eV}$  [39].

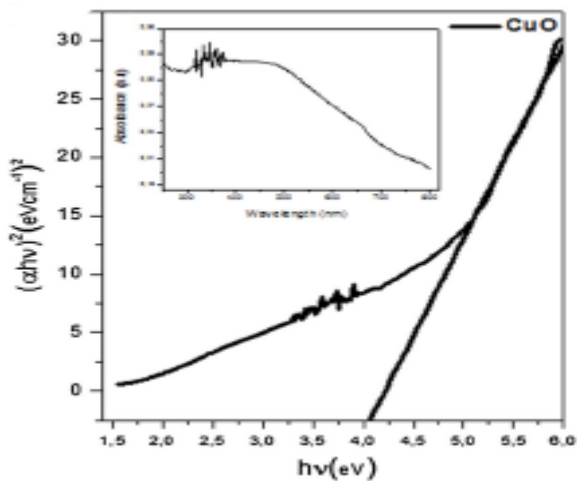


Figure 14. UV-Vis spectra and Tauc plots of CuO [39].

The result of another study using 3 samples, namely A, B, and C, was found that the particle size of CuO nanoparticles increasing with the calcination temperature. This is caused by the agglomeration of particles at high temperatures. The particle sizes of CuO A, B & C nanoparticles were 23, 25, and 28 nm. The reflectance appears above 830 nm for the three samples and the corresponding band gaps are 4.16, 4.17, and 4.16 eV for samples A, B, and C, respectively. From the SEM results, it appears that CuO nanoparticles become porous balls and the balls were aggregated with the calcination temperature [41].

The sol-gel method offers many advantages compared to other synthesis methods, such as particle size, has a high homogeneity of form, uses low raw materials, and can be produced on a large scale [42]. The sol-gel method can synthesize nanoparticle materials at room temperature, can produce most metals, and accurately control chemical and physical characteristics [24]. This method is the easiest method that requires low temperatures and is the most economical [40]. The sol-gel method is considered to have great potential for the manufacture of nanoparticles from copper and copper oxide [43]. This method is also free from toxic and hazardous materials [44]. The drawback of the sol-gel method is the relatively long time in the synthesis process [24].

#### IV.4. Green Synthesis Method

The synthesis of CuO nanoparticles can be carried out using the green synthesis method [25, 45-49] can be carried out using several reactants, namely a solution of copper (II) sulfate and leaf extract of *Ixora coccinea* [25], *Kalopanax pictum* [45], *Punica granatum* [46], *Abutilon indicum* [47],  $\text{CuCl}_2 \cdot 2\text{H}_2\text{O}$  and gum karaya [48], *Syzygium alternifolium* [49], and *Aloe vera* leaf extract and  $\text{Cu}(\text{NO}_3)_2$  [50]. An illustration of the synthesis of CuO nanoparticles is shown in Figure 16.

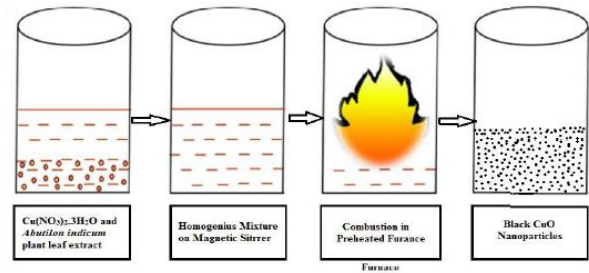


Figure 16. Illustration of the synthesis of CuO nanoparticles using the green synthesis method [47].

The preparation of plant extracts is done by collecting the leaves, cleaned, and cut into small pieces. The leaves are then washed with distilled water. The leaves are then stored in a measuring flask filled with water and kept in a heating mantle until boiling. Heating was stopped when the solution turned brown. The leaf extract was then cooled and filtered [25]. The synthesis process was carried out using a solution of copper (II) sulfate. A solution of copper(II) sulfate is a solution that has been stored overnight at room temperature so that bioreduction is possible and the copper salt is converted to copper oxide. The solution was centrifuged at 10,000 rpm using a 50 mL falcon tube for 20 minutes and washed several times with distilled water. Then the supernatant solution was discarded and the nanoparticles were transferred to another container. The obtained nanoparticles must be dried in an oven to remove the moisture content [25].

There is a direct correlation between pH value, salt concentration, polydispersity index, and CuO nanoparticle size with biological methods. The correlation depends on the concentration of  $\text{Cu}^{2+}$  ions in the solution, the enzymes released by the strain, and the pH of the solution. The results show the size distribution of the nanoparticles dispersed in the liquid to ensure the average size of the CuO nanoparticles. The polydispersity index measures the second moment of the nanoparticle population size distribution [25].

Nanoparticle characterization was carried out using several techniques including FT-IR, SEM, TEM [50], and UV-Vis spectrophotometer [25], and XRD (PAN). analytical equipment: XPERT-PRO).

SEM results revealed that CuO nanoparticles have a high tendency to agglomerate. From the analysis of the TEM images, it was found that CuO nanoparticles were concentrated at certain positions indicating their tendency to aggregate. The result of characterization by TEM result is shown in Figure 17.

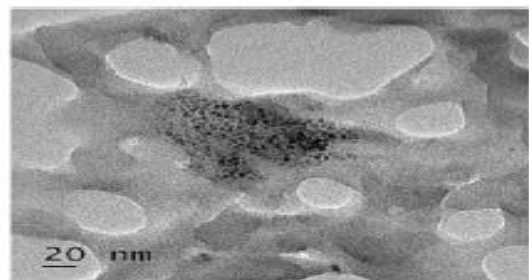


Figure 17. TEM results of synthesized CuO nanoparticles [25].

Characterization of CuO nanoparticles using a UV-Vis spectrophotometer, namely the UV spectrum of CuO nanoparticles showed an abnormal capacity of CuO nanoparticles to absorb UV light in the wavelength range from 200 to 300 nm. SEM results revealed the aggregation ability of CuO nanoparticles whereas TEM revealed the average CuO nanoparticle size had been reduced to 5 nm by sonication of nanoparticles in acetone base liquid. The result of characterization by UV-Vis spectrophotometer is shown in Figure 18.

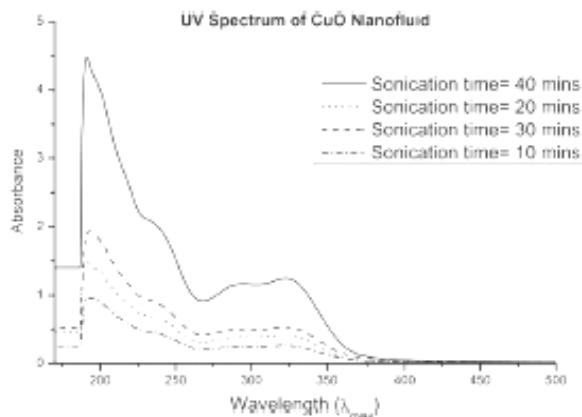


Figure 18. UV-Vis spectrum of CuO nanoparticles synthesized with various concentrations of leaf extract [25].

The FT-IR peak obtained at the time shows bond vibrations such as Cu-O and O-H in the CuO material. So that the synthesis of CuO nanoparticles using the green synthesis method was successfully carried out [25]. The results of characterization by FT-IR are shown in Figure 19.

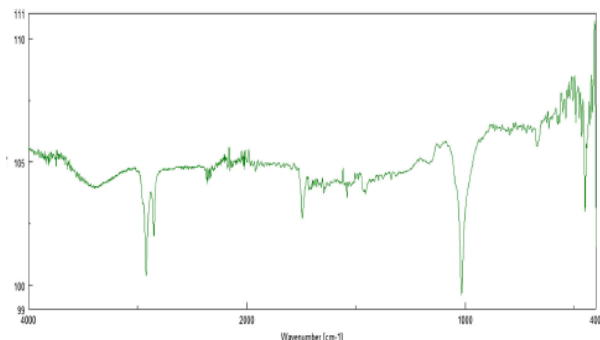


Figure 19. FT-IR spectrum of synthesized CuO nanoparticles [25].

The green synthesis method is more advantageous compared to other biological methods because it eliminates the use of cell culture and produces nanoparticles on a large scale [25]. The green synthesis method is also an environmentally friendly method with well-defined sizes, shapes, and mono dispersions [51]. The green synthesis method needs considerable attention because the protocol is cheaper than the basic synthetic method [52]. In addition, the green synthesis method has the ability as an antimicrobial agent against fish bacterial pathogens [50]. One of the disadvantages of this method is that the raw materials for the synthesis are relatively difficult to find [25].

#### IV.5. Hydrothermal Method

The hydrothermal method is a water-solvent heating process that involves heating the reactants in a closed container using water. In a closed container, the pressure increases and the water remains as a liquid. Heating water above its normal boiling point of 373 K is called superheated water. Conditions in which the pressure increases above atmospheric pressure are known as hydrothermal conditions. Hydrothermal synthesis is usually carried out at temperatures below 300 °C [29].

Sample preparation using the hydrothermal method was carried out without the use of surfactants [53]. The procedure in the synthesis of CuO nanoparticles by the hydrothermal method is to dissolve  $\text{Cu}(\text{CH}_3\text{COO})_2 \cdot \text{H}_2\text{O}$  4 g in 50 ml of water. Next, 40 mL of an aqueous solution of sodium hydroxybiogenicide (1 M/L) was added dropwise into the  $\text{Cu}(\text{CH}_3\text{COO})_2 \cdot \text{H}_2\text{O}$  solution. Then, 90 mL of the solution was transferred and sealed in a Teflon-coated stainless steel autoclave at 110 °C for 2 hours. Finally, the autoclave is removed and naturally cooled to room temperature. After the reaction stopped, the black precipitate was washed with deionized water and ethanol and then dried at 90 °C [26]. CuO nanoparticles can also be synthesized using  $\text{CuSO}_4 \cdot 5\text{H}_2\text{O}$  and NaOH. Where from these materials CuO powder will be produced which is stored in a vacuum desiccator to reduce the remaining solvent in the CuO powder [54].

The technique for characterizing CuO nanoparticles namely the size and morphology of the CuO nanostructures was examined by SEM (JEOL JSM-5900, Japan) connected to the attached EDS and the phase identification of the sample was examined by XRD (type Dmax III-A, Rigaku Co., Japan) using radiation. Cu-K $\alpha$  incidence, tube voltage 40 kV, and current 30 mA. The scanning range is from 20 to 60° 2 $\theta$  with a scan speed of 4°/min. The particle size was then calculated from the XRD spectrum using the Scherrer equation. The FT-IR spectra were recorded as KBr pellets using an ABB Bomen MB 100 spectrometer at wavenumbers between 400 and 4000  $\text{cm}^{-1}$ . The characterization technique is the XRD obtained on the Bruker D2 Phaser XRD system. Surface morphology by SEM was studied using a scanning electron microscope (JEOL JSM 840A) coupled with an energy dispersive X-ray analyzer (EDX) [55]. TEM and selected area diffraction patterns (SAED) were recorded using a Philips CM-200 instrument. Finally, FT-IR analysis was applied to determine the surface functional groups, using FT-IR spectroscopy (Bruker ATR), wherein the spectra were recorded from 400 to 4000  $\text{cm}^{-1}$  [56].

Figure 20 shows the XRD pattern of samples made by the hydrothermal process at 110 °C for 2 hours with different concentrations of copper acetate. All diffraction peaks can be indexed as monoclinic CuO phases with lattice constants  $a = 4.68\text{Å}$ ,  $b = 3.43\text{Å}$ ,  $c = 5.13\text{Å}$  and  $\beta = 99.26^\circ$  or  $99.47^\circ$  which, which is consistent with the values in standard card (JCPDS 80-0076 or JCPDS 05 0661), as previously reported. No other impurities were detected by XRD analysis, which indicates the phase

purity of the CuO nanostructures. And the main peaks located at  $2\theta = 35.5^\circ$  and  $38.7^\circ$  are indexed as crystal planes (0 0 2) and (1 1 1), respectively. The expansion of all the peaks recorded in the spectrum indicates the presence of nanoscale crystallites. In addition, with increasing  $\text{Cu}(\text{CH}_3\text{COO})_2$  concentration from 0.06 M/L to 0.7 M/L (from pattern 1a to pattern 1i), the diffraction peaks were highest and narrowest when the copper acetate concentration was 0.2 M/L, which illustrates that the crystallization and size of CuO nanostructures increase maximally [26].

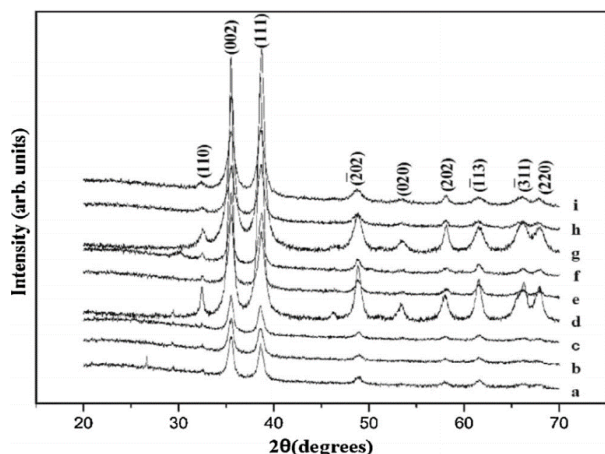


Figure 20. XRD pattern of CuO nanostructures made by hydrothermal approach at different concentrations of copper acetate: (a) 0.02 M/L, (b) 0.08 M/L, (c) 0.1 M/L, (d) 0.2 M/L, (e) 0.3 M/L, (f) 0.4 M/L, (g) 0.5 M/L, (h) 0.6 M/L, (i) 0.7 M/L [26].

The concentration of copper acetate used will affect the morphological size of the CuO nanoparticles, the greater the concentration of the reactant (Copper acetate), the greater the size of the CuO particles. The general morphology of the synthesized CuO products prepared by the hydrothermal route at different reactant concentrations was analyzed by FESEM and the results are shown in Figure 21 [22]. With the increase in the concentration of  $\text{Cu}(\text{CH}_3\text{COO})_2$ , the morphology of the CuO nanostructure has a large change. The floral morphology like CuO nanostructures was obtained at 0.4 M/L, as shown in Figure 21(a), which indicates that the flower-like CuO nanostructures are composed of irregular nanosheets about 70 nm wide and 1.7 μm long. With increasing reactant concentration, the morphology of the flower-like CuO nanostructures disappeared, and scattered plume-like nanosheets were formed, as shown in Figure 21(b). The nanoplate size is about 400 nm wide and 900 nm long. When the reactant concentration is equivalent to 0.6 M/L, the morphology changes to a spindle-like nanostructure. Thus, the morphology of CuO nanocrystals can be controlled by changing the concentration of the reactants [26].

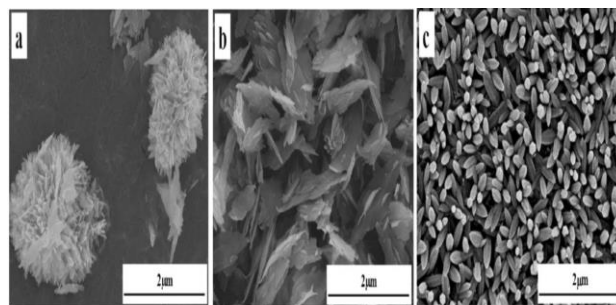


Figure 21. FESEM images of CuO nanostructures prepared under different concentrations of copper acetate at 110 °C for 2 hours: (a) 0.06 M/L, (b) 0.4 M/L, (c) 0.6 M/L [26].

Besides acting as a precipitate, NaOH is also very important in changing the shape of CuO particles. When NaOH is not used, the CuO particles produced are spherical, but when NaOH with a concentration of 1M is used, the resulting CuO particles form in layers. Figure 22 shows the morphology of the nanostructures grown with NaOH or not under the same conditions. When the synthesis process was carried out without NaOH, a Hericium erinaceus-like morphology of CuO was obtained, as shown in Figure 22(a). However, with increasing NaOH concentration to 1 M/L, there was a change in the morphology and layered structure of the CuO nanostructure, which we can conclude from Figure 22(b). That is, NaOH plays an important role to determine the morphology of CuO nanostructures because OH is strongly associated with reactions that form nanocrystals [26].

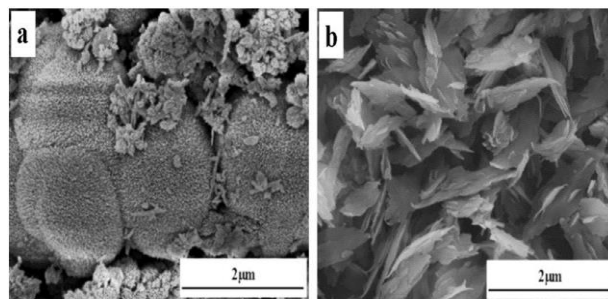


Figure 22. FESEM images of CuO nanostructures prepared with 0.4 M/L copper acetate at 110 °C for 2 hours: (a) without NaOH, (b) 1.0 M/L NaOH [26].

The effect of temperature will make the diffraction peaks higher and sharper, this will affect the size of the CuO particles. at a temperature of 110-140 °C CuO particle size is around 2000 nm, when the temperature is raised to 170 °C the CuO particles produced shrink to 500 nm. Figure 23 shows FESEM images of the synthesized CuO nanostructures made by the hydrothermal route at different temperatures. It can be seen that each of these lamellar structures. With increasing temperature, the morphology of CuO nanostructures changes slightly so that the nanosheet length becomes shorter, as shown in Figure 23(a-c). From Figure 23(d), we can see that when the hydrothermal temperature is up to 170 °C, CuO nanosheets are about 600 nm long and 200 nm wide [26].

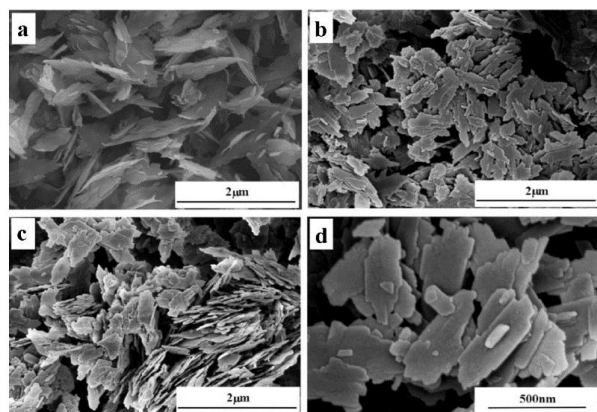


Figure 23. FESEM images of CuO nanostructures prepared at different reaction temperatures: (a) 110 °C, (b) 140 °C, low (c) and high magnification (d) images at 170 °C [26].

The final effect is the duration of the reaction, although this factor only slightly affects the results. By prolonging the reaction time, the resulting diffraction peaks will be higher and narrower, therefore the size of the CuO particles produced will be smaller. The morphology of the synthesized CuO products under different reaction times was observed using FESEM analysis and is shown in Figure 24. From low-magnification FESEM images of CuO nanosheets. Compared with the morphology of CuO nanosheets at 2 hours, the CuO nanostructures at 12 hours became clearer and had a smaller size. The reaction time has little influence on the morphology and structure of the product.

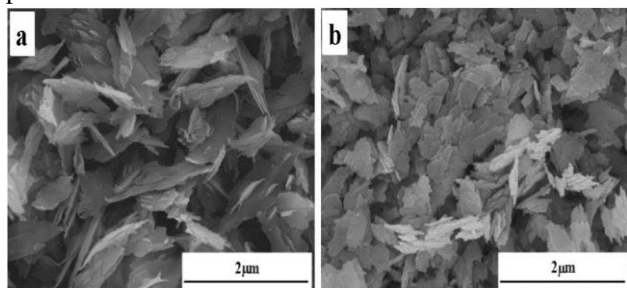


Figure 24. FESEM images of CuO nanostructures prepared under different reaction times (a) 2 h, (b) 12 h [26].

The hydrothermal method is an effective method to obtain the desired crystals, such as mild conditions, controlled morphology, low aggregation, and high crystallinity. In addition, the hydrothermal method is also relatively simple and easy to vary the variables of temperature, reactant concentration, and time on the growth of nanostructures [26]. In addition, the hydrothermal method can control the size and shape of the nanoparticles [29]. The disadvantages of this method are that it requires expensive equipment and it is difficult to control the stoichiometry of the solution [26]. Another disadvantage of the hydrothermal method is that hydrothermal slurries are corrosive, and the use of high-pressure vessels will be dangerous in the event of an accident [29].

#### IV.6. Biogenic Method

The biogenic method of CuO nanoparticles was prepared at room temperature by coprecipitation technique with several cation modifications. Briefly, in this experiment, 0.1 M solution of copper acetate  $\text{Cu}(\text{CH}_3\text{COO})_2 \cdot \text{H}_2\text{O}$  (purity 98.0%) and 40 mL plant extracts (such as algae) were stirred constantly for 30 minutes. Then, 0.2 M NaOH aqueous solution was added dropwise to the reaction mixture and allowed to stand for 4 hours. Next, the reaction solution was incubated overnight at room temperature for the deposition of the nanoparticles as a precipitate. The precipitate was separated by centrifugation at  $5000 \times g$  for 10 min, the precipitate was washed with deionized water, and dried at 80 °C for 12 h. CuO dry powder was calcined at 400 °C for 4 hours to obtain CuO nanoparticles [57]. After the nanoparticles are calcined, they are cooled to room temperature for further exploration through photocatalytic characterization and application [27].

According to the available literature, it was observed that the secondary moieties (alkaloids, flavonoids, polyphenols, and terpenoids) present in plant extracts tend to have a high enough potential to reduce the acetate group of metal salts through chelation [5]. Especially, the  $-\text{OH}$  group plays an important role in the synthesis of metal nanoparticles [58]. During the calcination process, the breaking of the bond between the metal salt and the  $-\text{OH}$  group causes the formation of metal oxide nanoparticles with the removal of water molecules [59-60]. A possible mechanism for the synthesis of CuO nanoparticles is described in Figure 25.

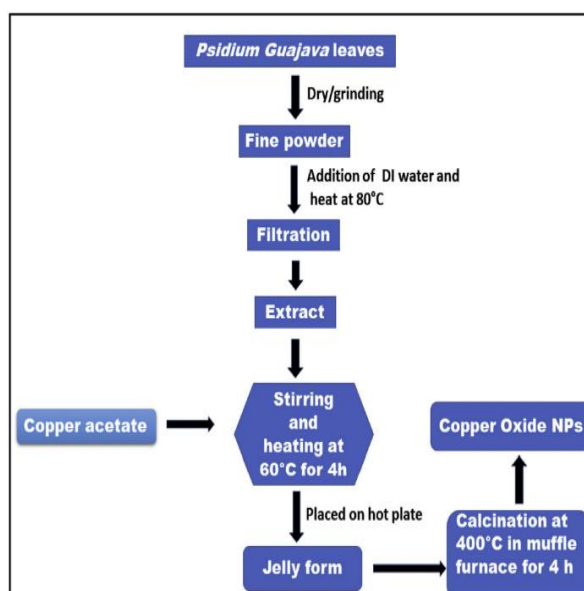


Figure 25. Schematic for stepwise synthesis procedure of CuO nanoparticles [27].

The functionality of the biogenic CuO nanoparticles was analyzed by the FT-IR. The morphology and size of the synthesized nanoparticles were measured using UV-vis, FE-SEM, and JEOL 2100 TEM. The elemental

composition of CuO nanoparticles was evaluated using XRD spectroscopy [27].

The ultraviolet-visible spectrum of the biogenic CuO nanoparticles synthesized with plant extracts is shown in Figure 26(a). The colloidal buffer of the final product showed a strong absorption band at 282 nm, which confirmed the formation of CuO nanoparticles. The absorption band at 282 nm is associated with the transition between the electron bands of the copper metal core present in the CuO nanoparticles [50]. The presence of protein-like molecules in the leaf extract is responsible for the reduction of Cu metal salts to form CuO nanoparticles [46]. The bandgap of the synthesized CuO nanoparticles was determined by the Tauc plot method [61], which involves plotting  $(\alpha h\nu)^{1/2}$  versus, as shown in Figure 26(b). In the Tauc plot,  $\alpha$  is the absorption coefficient and  $h\nu$  is the light energy. Furthermore,  $h$  is the Planck's constant of  $6.626 \times 10^{-34}$  Js [39].

XRD spectra of biogenic CuO nanoparticles showed a series of diffraction peaks at 32.63, 35.67, 38.78, 48.88, 58.34, 61.69, 68.16, and 75.32°. Which is associated with (110), (111), (202), (020), (113), (311), and (004) CuO monoclinic planes, respectively. The presence of a diffraction peak (between  $2\theta = 35\text{--}39^\circ$ ) confirmed the formation of CuO [62]. The XRD data obtained from the synthesized CuO nanoparticles are very similar to the monoclinic crystalline spectrum of CuO nanoparticles (eJCPDS 05 0661) which can be seen in Figure 26(c) [27].

FT-IR (Perkin Elmer, USA) was used to identify the functional groups present in CuO nanoparticles biosynthesized by the KBr pellet procedure. The visible-ultraviolet spectrum was measured from 200 to 600 nm in quartz using a UV-visible spectrophotometer (Model UV-2600, Shimadzu Inc. 01197). The surface functional groups of biogenic CuO nanoparticles were investigated by FT-IR spectroscopy. As shown in Figure 26(d), the spectrum of the synthesized CuO nanoparticles showed the main vibrational peaks at 530, 1088, 1628, 2842, and 3750  $\text{cm}^{-1}$ . The strong bands at 1088 and 530  $\text{cm}^{-1}$  are caused by CuO vibrations [50]. The 2842  $\text{cm}^{-1}$  band is due to the C=O alkanes of the proteins present on the surface of the nanoparticles, respectively. These bands are associated with protein residues present on the surface of the nanoparticles after the synthesis process. In this study, it was assumed that the protein present in the leaf extract was responsible for the reduction of the acetate group of metal salts to nanoparticles and acted as a stabilizing and capping agent for CuO nanoparticles [46]. FT-IR also suggested the presence of a hydroxyl group (band at 3750  $\text{cm}^{-1}$ ) on the surface of the synthesized CuO nanoparticles, which is thought to act as a stabilizer during the synthesis of biogenic CuO nanoparticles [46, 63-64].

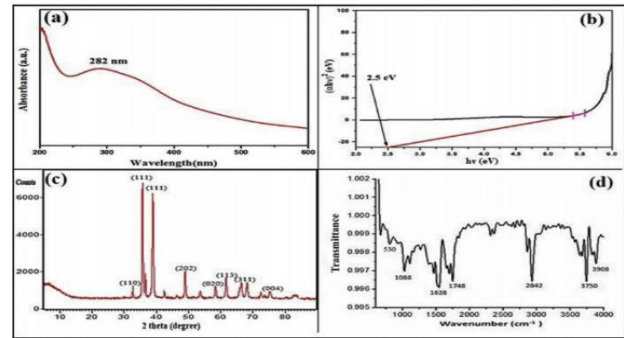


Figure 26. Spectral analysis of synthesized biogenic CuO nanoparticles: (a) UV vis, (b) Tauc plot, (c) XRD, and (d) FT-IR [27].

The morphological characteristics of the synthesized CuO nanoparticles were evaluated by FE-SEM. As shown in Figures 27(a and b), the nanoparticles exhibited a spherical morphology as coarse agglomerates. The same sample was used for EDX analysis. As shown in Figure 27(c), the agglomerated CuO nanoparticles contained 91.72 and 8.28% by weight Cu and O, respectively. The presence of other elements even from the leaf extract was negligible. Most of the remaining leaf extract molecules were removed during the washing and calcination processes of the synthesized nanoparticles CuO. However, due to the presence of carbon molecules in the leaf extract, a small amount of carbon may be present on the surface of the synthesized CuO nanoparticles in the form of capping [27]. As shown in Figure 28, the prepared CuO nanoparticles are spherical with a uniform size distribution of 2-6 nm [27].

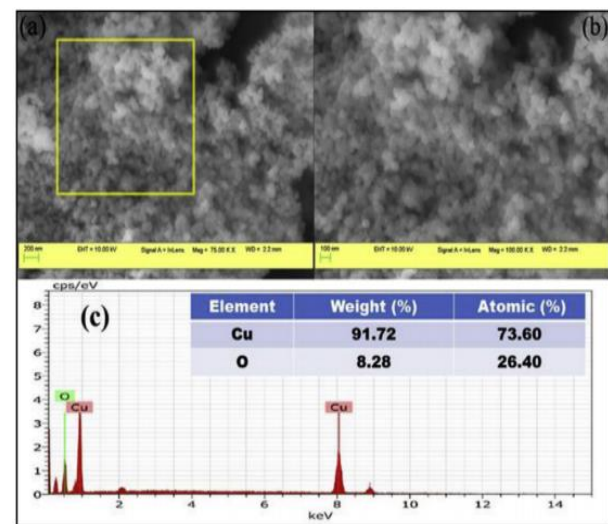


Figure 27. FE-SEM of synthesized biogenic CuO nanoparticles with (a) 200 nm (inset: square showing element mapping) and (b) 100 nm scale bars. Moreover, (c) for the EDX spectrum of CuO nanoparticles [27].

The specific surface area of the synthesized CuO nanoparticles was found to be 52.6  $\text{m}^2/\text{g}$  with a total pore volume of 0.197  $\text{cm}^3/\text{g}$  and an average pore diameter of 14.98 nm as described in Figure 28. S1 in Supplementary Information (SI). Note that all related information

referring to the Figure is also provided in the SI. The relative pressure ( $p/p_0$ ) is 0.985. In addition, the aggregation kinetics of CuO nanoparticles has been investigated through a particle size analyzer using NaCl as an electrolyte at different concentrations (20, 40, and 60 mM) [65]. A very small change in mean particle size was observed even at 60 mM NaCl concentration. Similarly, control experiments (without NaCl) showed negligible variation in particle size after 60 min which signifies stability of the synthesized nanoparticles.

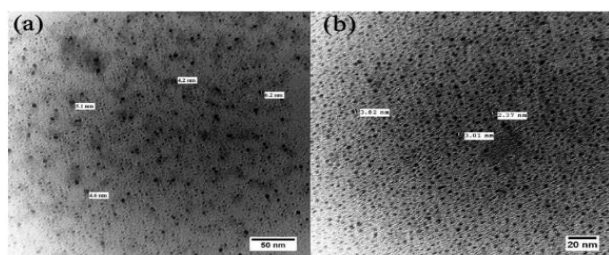


Figure 28. TEM micrograph of synthesized CuO nanoparticles: (a) 50 nm and (b) 20 nm scale rods [27].

There are advantages to this method, namely the procedure is simple, the equipment required is environmentally friendly, and does not require high costs. However, this method also has drawbacks, namely the difficulty of implementing on a large scale and the need to maintain cell cultures and it is difficult to control the size, shape, and crystallinity [27].

## V. Conclusion

CuO nanoparticles are oxide semiconductors that have unique properties and have many applications in several fields and are useful in everyday life. One of its uses is that it can be used to divert heat energy. The addition of a volume of CuO nanoparticles into the nitrate salt can increase the thermal diffusivity and thermal conductivity used in solar power plants. CuO nanoparticles can be synthesized from several methods: (1) electrochemistry, (2) sonochemistry, (3) sol-gel, (4) green synthesis, (5) hydrothermal, and (6) biogenic methods. Each method has its results and advantages. Among the methods described, the hydrothermal method is the most effective and efficient method for industrial scale. This is because the method is simple (without using any surfactant template), it is easy to vary the variables of temperature, reactant concentration, and time on the growth of nanostructures. This paper is expected to provide some considerations regarding the synthesis method of CuO nanoparticles that can be used on an industrial scale based on the advantages of each method.

## Acknowledgments

We acknowledged Bangdos Universitas Pendidikan Indonesia.

## References

- [1] N. T. Rochman, Y. L. Brama, "Indonesia nanotechnology development: current status overview", In *Emerging Nanotechnology Power: Nanotechnology R&D and Business Trends in the Asia Pacific Rim*, 2019, pp. 141-167.
- [2] S. Saravanan and T. Sivasankar, "Effect of ultrasound power and calcination temperature on the sonochemical synthesis of copper oxide nanoparticles for textile dyes treatment", *Environmental Progress & Sustainable Energy*, Vol 35, Issue 3, May 2016, pp. 669-679.
- [3] T. Velusamy, A. Liguori, M. Macias-Montero, D. B. Padmanaban, D. Carolan, M. Gherardi, V. Colombo, P. Maguire, V. Svrcek, D. Mariotti, "Ultra-small CuO nanoparticles with tailored energy-band diagram synthesized by a hybrid plasma-liquid process", *Plasma Processes and Polymers*, Vol 14, Issue 7, February 2017, pp. 1-8.
- [4] N. Dighore, S. Jadhav, S. Gaikwad, A. Rajbhoj, "Copper oxide nanoparticles synthesis by electrochemical method", *Materials Science*, Vol 22, Issue 2, June 2016, pp. 170-173.
- [5] B. Naseer, G. Srivastava, O. S. Qadri, S. A. Faridi, R. U. Islam, K. Younis, "Importance and health hazards of nanoparticles used in the food industry", *Nanotechnology Reviews*, Vol 7, Issue 6, December 2018, pp. 623-641.
- [6] Jr. P. D. Myers, T. E. Alam, R. Kamal, D. Y. Goswami, E. Stefanakos, "Nitrate salts doped with CuO nanoparticles for thermal energy storage with improved heat transfer", *Applied Energy*, Vol 165, March 2016, pp. 225-233.
- [7] K. Borgohain, J. B. Singh, M. R. Rao, T. Shripathi, S. Mahamuni, "Quantum size effects in CuO nanoparticles", *Physical Review B*, Vol 61, Issue 16, April 2000, pp. 94-96.
- [8] N. Silva, S. Ramires, I. Diaz, A. Garcia, N. Hassan, "Easy, quick, and reproducible sonochemical synthesis of CuO nanoparticles", *Materials*, Vol 12, Issue 5, January 2019, pp. 804.
- [9] S. Moleh, M. R. Rahimi, M. Ghaedi, K. Dashtian, S. Hajati, "Sonochemical-assisted synthesis of CuO/Cu<sub>2</sub>O/Cu nanoparticles as efficient photocatalyst for simultaneous degradation of pollutant dyes in rotating packed bed reactor: LED illumination and central composite design optimization", *Ultrasonics sonochemistry*, Vol 40, January 2018, pp. 601-610.
- [10] E. Mousali, M. A. Zanjachi, "Electrochemical synthesis of copper (II) oxide nanorods and their application in photocatalytic reactions", *Journal of Solid State Electrochemical*, Vol 23, Issue 3, March 2019, pp. 925-935.
- [11] I. M. Araújo, R. R. Silva, G. Pacheco, W. R. Lustrri, A. Tercejak, J. Gutierrez, J. R. S. Júnior, F. H. C. Azevedo, G. S. Figüredo, M. L. Vega, S. J. L. Ribeiro, H.S. Barud, "Hydrothermal synthesis of bacterial cellulose-copper oxide nanocomposites and evaluation of their antimicrobial activity", *Carbohydrate polymers*, Vol 179, Issue 3, January 2018, pp. 341-349.
- [12] S. Jadhav, S. Gaikwad M. Nimse, A. Rajbhoj, "Copper oxide nanoparticles: synthesis, characterization and their antibacterial activity", *Journal of Cluster Science*, Vol 22, Issue 2, June 2011, pp. 121-129.
- [13] N. C. Joshi, Y. A. S. H. W. A. N. I. Prakash, "Leaves extract-based biogenic synthesis of cupric oxide nanoparticles, characterizations, and antimicrobial

- activity”, *Asian J Pharm Clin Res*, Vol 12, Issue 8, 2019, pp. 288-291.
- [14] P. Pandey, S. Merwyn, G. S. Agarwal, B. K. Tripathi, S. C. Pant, “Electrochemical synthesis of multi-armed CuO nanoparticles and their remarkable bactericidal potential against waterborne bacteria”, *Journal of Nanoparticle Research*, Vol 14, Issue 1, January 2012, pp. 1-13.
- [15] G. Sharmila, R. S. Pradeep, K. Sandiya, S. Santhiya, C. Muthukumaran, J. Jeyanthi, N. M. Kumar, M. Thirumarimurugan, “Biogenic synthesis of CuO nanoparticles using *Bauhinia tomentosa* leaves extract: characterization and its antibacterial application”, *Journal of Molecular Structure*, Vol 1165, August 2018, pp. 288-292.
- [16] R. Sivaraj, P. K. Rahman, P. Rajiv, H. A. Salam, R. Venckatesh, “Biogenic copper oxide nanoparticles synthesis using *Tabernaemontana divaricate* leaf extract and its antibacterial activity against urinary tract pathogen”, *Spectrochimica Acta Part A: Molecular and Biomolecular Spectroscopy*, Vol 133, December 2014, pp. 178-181.
- [17] V. V. Khedekar, B. M. Bhanage, “Simple electrochemical synthesis of cuprous oxide nanoparticles and their application as a non-enzymatic glucose sensor”, *Journal Of the Electrochemical Society*, Vol 163, Issue 6, March 2016, B248.
- [18] J. Zhang, J. Wang, Y. Fu, B. Zhang, Z. Xie, “Sonochemistry-synthesized CuO nanoparticles as an anode interfacial material for efficient and stable polymer solar cells”, *Rsc Advances*, Vol 5, Issue 36, 2015, pp. 28786-28793.
- [19] H. Abbasian, D. Ghanbari, G. Nabiyouni, “Sonochemical-assisted synthesis of copper oxide nanoparticles and its application as humidity sensor”, *Journal of NANOSTRUCTURES*, Vol 3, Issue 4, December 2013, pp. 429-434.
- [20] Z. Zhong, V. Ng, J. Luo, S. P. Teh, J. Teo, A. Gedanken, “Manipulating the self-assembling process to obtain control over the morphologies of copper oxide in hydrothermal synthesis and creating pores in the oxide architecture”, *Langmuir*, Vol 23, Issue 11, May 2007, pp. 5971-5977.
- [21] S. Bhuvaneshwari, N. Gopalakrishnan, “Hydrothermally synthesized Copper Oxide (CuO) superstructures for ammonia sensing”, *Journal of colloid and interface science*, Vol 480, October 2016, pp. 76-84.
- [22] M. A. Choudhary, R. Manan, M. M. Aslam, K. H. Rashid, S. Qayyum, Z. Ahmed, “Biogenic Synthesis of Copper oxide and Zinc oxide Nanoparticles and their Application as Antifungal Agents”, *Int. J. Mater. Sci. Eng*, Vol 4, 2018, pp. 1-6.
- [23] N. Wongpisutpaisan, P. Charoonsuk, N. Vittayakorn, W. Pecharapa, “Sonochemical synthesis and characterization of copper oxide nanoparticles”, *Energy Procedia*, Vol 9, January 2011, pp. 404-409.
- [24] H. K. Thanoon, K. A. Hubeatir, A. A. Al-Amiery, “Synthesis of copper oxide nanoparticles via sol-gel method”, *International Journal of Research in Engineering and Innovation*, Vol 1, Issue 4, 2017, pp. 43-45.
- [25] K. Vishveshvar, M. A. Krishnan, K. Haribabu, S. Vishnuprasad, “Green synthesis of copper oxide nanoparticles using *Ixiro coccinea* plant leaves and its characterization”, *BioNanoScience*, Vol 8, Issue 2, June 2018, pp. 554-558.
- [26] T. Jiang, Y. Wang, D. Meng, X. Wu, J. Wang, J. Chen, “Controllable fabrication of CuO nanostructure by hydrothermal method and its properties”, *Applied Surface Science*, Vol 3, Issue 11, August 2014, pp. 602-608.
- [27] J. Singh, V. Kumar, K. H. Kim, M. Rawat, M., “Biogenic synthesis of copper oxide nanoparticles using plant extract and its prodigious potential for photocatalytic degradation of dyes”, *Environmental research*, Vol 177, October 2019, pp. 108569.
- [28] N. Verma, N. Kumar, “Synthesis and biomedical applications of copper oxide nanoparticles: an expanding horizon”, *ACS Biomaterials Science & Engineering*, Vol 5, Issue 3, February 2019, pp. 1170-1188.
- [29] S. K. W. Ningsih, “Sintesis Anorganik. Padang”, UNP Press, 2016, 76-99
- [30] H. Yang, J. Ouyang, A. Tang, Y. Xiao, X. Li, X. Dong, Y. Yu, “Electrochemical synthesis and photocatalytic property of cuprous oxide nanoparticles”, *Materials Research Bulletin*, Vol 41, Issue 7, July 2006, pp. 1310-1318.
- [31] S. M. Pourmortazavi, M. Rahimi-Nasrabadi, A. Sobhani-Nasab, M. S. Karimi, M. R. Ganjali, S. Mirsadeghi, “Electrochemical synthesis of copper carbonates nanoparticles through experimental design and the subsequent thermal decomposition to copper oxide”, *Materials Research Express*, Vol 6, Issue 4, January 2019, pp. 045065.
- [32] M. Starowicz, M., “Electrochemical synthesis of copper oxide particles with controlled oxidation state, shape and size”, *Materials Research Express*, Vol 6, Issue 8, May 2019, 0850a3.
- [33] N. A. Neto, P. M. Oliveira, R. M. Nascimento, C. A. Paskocimas, M. R. D. Bomio, F. V. Motta, “Influence of pH on the morphology and photocatalytic activity of CuO obtained by the sonochemical method using different surfactants”, *Ceramics International*, Vol 45, Issue 1, January 2019, pp. 651-658.
- [34] R. Ranjbar-Karimi, A. Bazmandegan-Shamili, A. Aslani, K. Kaviani, K., “Sonochemical synthesis, characterization and thermal and optical analysis of CuO nanoparticles”, *Physica B: Condensed Matter*, Vol 405, Issue 15, August 2010, pp. 3096-3100.
- [35] S. Anandan, G. J. Lee, J. J. Wu, “Sonochemical synthesis of CuO nanostructures with different morphology”, *Ultrasonics sonochemistry*, Vol 19, Issue 3, May 2012, pp. 682-686.
- [36] Y. Aparna, K. E. Rao, P. S. Subbarao, “Synthesis and characterization of CuO nano particles by novel sol-gel method”, In *Proceedings of the 2nd International Conference on Environment Science and Biotechnology*, Vol 48, 2012, pp. 156-160.
- [37] B. Arunkumar, S. J. Jeyakumar, M. Jothibas, M., “A sol-gel approach to the synthesis of CuO nanoparticles using *Lantana camara* leaf extract and their photo catalytic activity”, *Optik*, Vol 183, April 2019, pp. 698-705.
- [38] J. Jayaprakash, N. Srinivasan, P. Chandrasekaran, E. K. Girija, “Synthesis and characterization of cluster of grapes like pure and Zinc-doped CuO nanoparticles by sol-gel method”, *Spectrochimica Acta Part A: Molecular and Biomolecular Spectroscopy*, Vol 136, February 2015, pp. 1803-1806.
- [39] N. Zayyoun, L. Bahmad, L. Laânab, B. Jaber, “The effect of pH on the synthesis of stable Cu<sub>2</sub>O/CuO nanoparticles by sol-gel method in a glycolic medium”, *Applied Physics A*, Vol 122, Issue 5, May 2016, pp. 488.
- [40] Z. N. Kayani, M. Umer, S. Riaz, S. Naseem, “Characterization of copper oxide nanoparticles fabricated

- by the sol-gel method”, *Journal of Electronic Materials*, Vol 44, Issue 10, October 2015, pp. 3704-3709.
- [41] K. Nithya, P. Yuvaree, N. Neelakandeswari, N. Rajasekaran, K. Uthayarani, M. Chitra, S. S. Kumar, “Preparation and characterization of copper oxide nanoparticles”, *Int. J. ChemTech Res*, Vol 6, Issue 3, May 2014, pp. 2220-2222.
- [42] H. Siddiqui, M. R. Parra, F. Z. Haque, “Optimization of process parameters and its effect on structure and morphology of CuO nanoparticle synthesized via the sol-gel technique”, *Journal of Sol-Gel Science and Technology*, Vol 87, Issue 1, July 2018, pp. 125-135.
- [43] O. Akhavan, H. Tohidi, A. Z. Moshfegh “Synthesis and electrochromic study of sol-gel cuprous oxide nanoparticles accumulated on silica thin film”, *Thin Solid Films*, Vol 517, Issue 24, October 2009, pp. 6700-6706.
- [44] M. Altikatoglu, A. Attar, F. Erci, C.M. Cristache, I. Isildak, “Green synthesis of copper oxide nanoparticles using *Ocimum basilicum* extract and their antibacterial activity”, *Fresenius Environ. Bull*, Vol 25, January 2017, pp. 7832-7837.
- [45] S.A. Akintelu, A.S. Folorunso, F.A. Folorunso, A.K. Oyebamiji, “Green synthesis of copper oxide nanoparticles for biomedical application and environmental remediation”, *Heliyon*, Vol 6, Issue 7, July 2020, pp. e04508.
- [46] A. Y. Ghidan, T. M. Al-Antary, A.M. Awwad, “Green synthesis of copper oxide nanoparticles using *Punica granatum* peels extract: Effect on green peach Aphid”, *Environmental Nanotechnology, Monitoring & Management*, Vol 6, December 2016, pp. 95-98.
- [47] F. Ijaz, S. Shahid, S.A. Khan, W. Ahmad, S. Zaman, “Green synthesis of copper oxide nanoparticles using *Abutilon indicum* leaf extract: Antimicrobial, antioxidant and photocatalytic dye degradation activities”, *Tropical Journal of Pharmaceutical Research*, Vol 16, Issue 4, May 2017, pp. 743-753.
- [48] V. V. T. Padil and M. Černík, “Green synthesis of copper oxide nanoparticles using gum karaya as a biotemplate and their antibacterial application”, *International journal of nanomedicine*, Vol 8, February 2013, pp. 889-898
- [49] P. Yugandhar, T. Vasavi, P.U.M. Devi, N. Savithamma, “Bioinspired green synthesis of copper oxide nanoparticles from *Syzygium alternifolium* (Wt.) Walp: characterization and evaluation of its synergistic antimicrobial and anticancer activity”, *Applied Nanoscience*, Vol 7, Issue 7, October 2017, pp. 417-427.
- [50] P. V. Kumar, U. Shameem, P. Kollu, R.L. Kalyani, S.V.N. Pammi, “Green synthesis of copper oxide nanoparticles using *Aloe vera* leaf extract and its antibacterial activity against fish bacterial pathogens”, *BioNanoScience*, Vol 5, Issue 3, September 2015, pp. 135-139.
- [51] S. Honary, H. Barabadi, E. Gharaei-Fathabad, F. Naghibi, “Green synthesis of copper oxide nanoparticles using *Penicillium aurantiogriseum*, *Penicillium citrinum* and *Penicillium waksmanii*”, *Dig J Nanomater Bios*, Vol 7, Issue 3, July 2012, pp. 999-1005.
- [52] D. Berra, S.E. Laouini, B. Benhaoua, M.R. Ouahrani, D. Berrani, A. Rahal, “Green synthesis of copper oxide nanoparticles by *Phoenix dactylifera* L leaves extract”, *Digest Journal of Nanomaterials and Biostructures*, Vol 13, Issues 4, October 2018, pp. 1231-1238.
- [53] K.J. Arun, A.K. Batra, A. Krishna, K. Bhat, M.D. Aggarwal, P.J. Francis, “Surfactant free hydrothermal synthesis of copper oxide nanoparticles”, *Am. J. Mater. Sci*, Vol 5, 2015, pp. 36-38.
- [54] B. Dutta, E. Kar, N. Bose, S. Mukherjee, “Significant enhancement of the electroactive  $\beta$ -phase of PVDF by incorporating hydrothermally synthesized copper oxide nanoparticles”, *RSC advances*, Vol 5, Issues 127, November 2015, pp. 105422-105434.
- [55] K.Y. Kumar, H.B. Muralidhara, Y.A. Nayaka, H. Hanumanthappa, M. S. Veena, S. K. Kumar, “Hydrothermal synthesis of hierarchical copper oxide nanoparticles and its potential application as adsorbent for Pb (II) with high removal capacity”, *Separation Science and Technology*, Vol 49, Issues 15, October 2015, pp. 2389-2399.
- [56] M.P. Neupane, Y.K. Kim, I.S. Park, K.A. Kim, M.H. Lee, T.S. Bae, “Temperature driven morphological changes of hydrothermally prepared copper oxide nanoparticles”, *Surface and Interface Analysis: An International Journal devoted to the development and application of techniques for the analysis of surfaces, interfaces and thin films*, Vol 41, Issues 3, January 2009, pp. 259-263.
- [57] D. Vinu, K. Govindaraju, R. Vasantharaja, S.A. Nisa, M. Kannan, K.V. Anand, “Biogenic zinc oxide, copper oxide and selenium nanoparticles: preparation, characterization and their anti-bacterial activity against *Vibrio parahaemolyticus*”, *Journal of Nanostructure in Chemistry*, Vol 11, Issue 2, June 2021, pp. 271-286.
- [58] M. Imran Din and A. Rani, “Recent advances in the synthesis and stabilization of nickel and nickel oxide nanoparticles: a green adeptness”, *International journal of analytical chemistry*, June 2016.
- [59] S. Kaur, J. Singh, R. Rawat, S. Kumar, H. Kaur, K.V. Rao, M. Rawat, “A smart LPG sensor based on chemo-bio synthesized MgO nanostructure”, *Journal of Materials Science: Materials in Electronics*, Vol 29, Issues 14, July 2018, pp. 11679-11687.
- [60] A. Singh, N.B. Singh, I. Hussain, H. Singh, V. Yadav, “Synthesis and characterization of copper oxide nanoparticles and its impact on germination of *Vigna radiata* (L.) R. Wilczek”, *Tropical Plant Research*, Vol 4, Issue 2, June 2017, pp. 246-253.
- [61] B.D. Vierzicke, “Investigation of L-cystine assisted Cu<sub>3</sub>BiS<sub>3</sub> synthesis for energetically and environmentally improved integration as thin-film solar cell p-type semiconductor absorber”, *Rutgers The State University of New Jersey-New Brunswick*, January 2015.
- [62] A. Nezamzadeh-Ejehieh and S. Hushmandrad, “Solar photodecolorization of methylene blue by CuO/X zeolite as a heterogeneous catalyst”, *Applied Catalysis A: General*, Vol 388, Issues 1-2, November 2010, pp. 149-159.
- [63] A. Nezamzadeh-Ejehieh and M. Karimi-Shamsabadi, “Decolorization of a binary azo dyes mixture using CuO incorporated nanozeolite-X as a heterogeneous catalyst and solar irradiation”, *Chemical engineering journal*, Vol 228, July 2012, pp. 631-641.
- [64] S. Senobari and A. Nezamzadeh-Ejehieh, “A pn junction NiO-CdS nanoparticles with enhanced photocatalytic activity: a response surface methodology study”, *Journal of Molecular Liquids*, Vol 257, May 2018, pp. 173-183.
- [65] V.S. Sousa and M.R. Teixeira, “Aggregation kinetics and surface charge of CuO nanoparticles: the influence of pH, ionic strength and humic acids”, *Environmental Chemistry*, Vol 10, Issue 4, August 2013, pp. 313-322.